Global-Scale Similarities in Nitrogen Release Patterns During Long-Term Decomposition

William Parton, *et al.*

Science **315**, 361 (2007);
DOI: 10.1126/science.1134853

Science (print ISSN 0036-8075; online ISSN 1095-9203) is published weekly, except the last week in December, by the American Association for the Advancement of Science, 1200 New York Avenue NW, Washington, DC 20005.

14. K. M. Sung, D. W. Mosley, B. R. Peelle, S. G. Zhang, J. M. Jacobson, *J. Am. Chem. Soc.* **126**, 5064 (2004).
15. J. G. Worden, A. W. Shaffer, Q. Huo, *Chem. Commun.* **2004**, 518 (2004).
16. F. W. Huo, A. K. R. Lytton-Jean, C. A. Mirkin, *Adv. Mater.* **18**, 2304 (2006).
17. D. R. Nelson, *Nano Lett.* **2**, 1125 (2002).
18. A. M. Jackson, J. W. Myerson, F. Stellacci, *Nat. Mater.* **3**, 330 (2004).
19. J. C. Love, L. A. Estroff, J. K. Kriebel, R. G. Nuzzo, G. M. Whitesides, *Chem. Rev.* **105**, 1103 (2005).
20. F. Schreiber, *Prog. Surf. Sci.* **65**, 151 (2000).
21. W. D. Luedtke, U. Landman, *J. Phys. Chem. B* **102**, 6566 (1998).
22. H. Poincare, *J. Math Pure Appl.* **1**, 167 (1885).
23. M. Eisenberg, R. Guy, *Am. Math. Mon.* **86**, 571 (1979).
24. A. M. Jackson, Y. Hu, P. J. Silva, F. Stellacci, *J. Am. Chem. Soc.* **128**, 11135 (2006).
25. R. K. Smith *et al.*, *J. Phys. Chem. B* **105**, 1119 (2001).
26. The one-phase chaining reaction is less efficient than the two-phase reaction for many reasons: Mainly, it is challenging to get the exact stoichiometric ratio of nanoparticles to divalent molecules. The kinetics of the polymerization reaction are also slower. However, the one-phase reaction product can be directly cast onto TEM grids from solution with no intermediate processing, and consequently it can be quantitatively analyzed.
27. M. J. Hostetler, A. C. Templeton, R. W. Murray, *Langmuir* **15**, 3782 (1999).
28. Y. Song, R. W. Murray, *J. Am. Chem. Soc.* **124**, 7096 (2002).
29. R. L. Donkers, Y. Song, R. W. Murray, *Langmuir* **20**, 4703 (2004).
30. As determined by timed experiments. The amount of pole-functionalized nanoparticles that precipitate can be measured through optical spectroscopy of the organic phase in the two-phase polymerization system. See SOM Materials and Methods for details.
31. The authors are grateful to V. Vitelli and D. Nelson for helpful discussions. The financial support of the National Science Foundation (Nanotechnology Interdisciplinary Research Team Division of Materials Research-0303973) and of the Petroleum Research Foundation are acknowledged. F.S. is grateful to 3M, DuPont, and the Packard Foundation for the young faculty awards. G.A.D. acknowledges support from the Department of Defense National Defense Science and Engineering Graduate Fellowship, and A.M.J. from the Collamore Fellowship for graduate students. This work made use of the shared facilities of the Material Research Science and Education Center Program of the National Science Foundation under award DMR 02-13282.

Supporting Online Material

www.sciencemag.org/cgi/content/full/315/5810/358/DC1
Materials and Methods
SOM Text
Figs. S1 to S7
References

28 July 2006; accepted 6 December 2006
10.1126/science.1133162

Global-Scale Similarities in Nitrogen Release Patterns During Long-Term Decomposition

William Parton,[1] Whendee L. Silver,[2] Ingrid C. Burke,[1,3] Leo Grassens,[4] Mark E. Harmon,[5] William S. Currie,[6] Jennifer Y. King,[7] E. Carol Adair,[8] Leslie A. Brandt,[8] Stephen C. Hart,[9] Becky Fasth[5]

Litter decomposition provides the primary source of mineral nitrogen (N) for biological activity in most terrestrial ecosystems. A 10-year decomposition experiment in 21 sites from seven biomes found that net N release from leaf litter is dominantly driven by the initial tissue N concentration and mass remaining regardless of climate, edaphic conditions, or biota. Arid grasslands exposed to high ultraviolet radiation were an exception, where net N release was insensitive to initial N. Roots released N linearly with decomposition and exhibited little net N immobilization. We suggest that fundamental constraints on decomposer physiologies lead to predictable global-scale patterns in net N release during decomposition.

Litter decomposition converts the products of photosynthesis to inorganic components and stable soil organic matter. Decomposition releases more carbon (C) annually than fossil fuel combustion (*1*, *2*), and it represents the primary source of nutrients for plants, and both nutrients and energy for microbes, over biological time scales (*3*, *4*). This is particularly true for the supply of nitrogen (N), which lacks a notable geologic input and is commonly a limiting element to plant growth (*5*). Internal recycling of N from litter decomposition thus provides a key resource for ecosystem productivity.

Litter decomposition is a lengthy process generally requiring years to decades for completion, and considerable N remains in litter after the initial decomposition phase (*6*–*8*). The vast majority of decomposition studies have been conducted over short time periods (<5 years), and at local scales using site-specific litters (*9*–*11*), making cross-site comparisons difficult. The lack of long-term broad-scale studies on litter decomposition and nutrient release inhibits our ability to accurately predict ecosystem C balance and response to environmental change at regional and global scales. The Long-Term Intersite Decomposition Experiment (LIDET) was a 10-year effort encompassing most of the world's biomes designed to determine long-term controls on decomposition and nutrient immobilization or mineralization. The study used several leaf and root litters that differed in chemical quality, with a core set of five to six leaf litters and three root litters that were decomposed at all sites (*12*). This data set is unique in that it encompasses the global array of climatic conditions (Table 1), includes a wide range of soil types and associated soil microbial community compositions, and was carried out over an unprecedented time span. Our goal was to use the LIDET core litter data set (*1*) from upland terrestrial sites to determine which combination of climate, initial litter chemistry, and site-specific characteristics (e.g., those derived from edaphic conditions and decomposer biota) best predict long-term patterns in litter N dynamics during decomposition (*1*, *10*, *12*–*14*). The data set included seven biomes, each with at least two replicate sites (n = 21 sites). We used mean annual temperature and precipitation, actual evapotranspiration, and the climatic decomposition index (CDI) as potential predictors of decomposition rates and N dynamics (Table 1). The CDI incorporates seasonality in temperature and moisture and has been shown to be well correlated with decomposition rates over 1 to 5 years (*1*). The core litters were chosen to encompass a wide range of C:N ratios, and concentrations of N, lignin, and other secondary compounds (Table 1, table S2).

CDI was the best predictor of decomposition rates globally (correlation coefficient r^2 = 0.68). Leaf and root litter decomposition were slowest in the cold, dry regions, such as boreal forest and tundra, and fastest in the warm, moist tropical forests (Fig. 1). A notable exception was the rapid leaf litter decomposition rate in arid-zone perennial grasslands despite a CDI of 0.11 (Fig. 1C); these ecosystems may have been affected by ultraviolet (UV) radiation (*15*–*17*) in addition to climate.

Unlike patterns in mass loss, net N immobilization and release in leaf litter were strongly

[1]Natural Resource Ecology Laboratory, Colorado State University, 200 West Lake, Campus Mail 1499, Fort Collins, CO 80523–1499, USA. [2]Ecosystem Science Division, Department of Environmental Science, Policy, and Management, 137 Mulford Hall #3114, University of California, Berkeley, CA 94720, USA. [3]Department of Forest, Rangeland, and Watershed Stewardship, and Graduate Degree Program in Ecology, Colorado State University, Fort Collins, CO 80523–1472, USA. [4]LSI Logic Inc., 1636 Southwest 26th Street, Loveland, CO 80227, USA. [5]Department of Forest Science, Oregon State University, Corvallis, OR 97331, USA. [6]School of Natural Resources and Environment, University of Michigan, Ann Arbor, MI 48103, USA. [7]Department of Soil, Water, and Climate and Department of Ecology, Evolution, and Behavior, University of Minnesota, 439 Borlaug Hall, 1991 Upper Buford Circle, St. Paul, MN 55108, USA. [8]Department of Ecology, Evolution, and Behavior, University of Minnesota, 100 Ecology Building, 1987 Upper Buford Circle, St. Paul, MN 55108, USA. [9]School of Forestry and Merriam-Powell Center for Environmental Research, Northern Arizona University, Flagstaff, AZ 86011, USA.

Table 1. Climate data for the seven biomes used in this study. The mean time to the initiation of net N release (TNET) is given in years for each leaf litter species and biome and was calculated using the best-fit equation to determine the point of maximum net N immobilization (*18*). Mean precipitation (PPT), temperature (TMP), actual evapotranspiration (AET), and the climatic decomposition index (*37*) are shown. TRAE, *Triticum aestivum*; PIRE, *Pinus resinosa*; THPL, *Thuja plicata*; ACSA, *Acer saccharum*; QUPR, *Quercus prinus*; DRGL, *Drypetes glauca*.

Biome	Mean annual PPT (mm)	Mean annual TMP (°C)	Climatic decomposition index (CDI)	Mean AT (mm)	TRAE 0.38% N TNET	PIRE 0.58% N TNET	THPL 0.62% N TNET	ACSA 0.80% N TNET	QUPR 1.02% N TNET	DRGL 1.98% N TNET
Arid grassland	331	13.0	0.11	1490	–	–	–	–	–	–
Humid grassland	807	9.8	0.30	1138	3.5	3	3.9	1.75	1.6	0.25
Tundra	788	−6.0	0.09	589	9.5	7.6	6.4	2.6	1.6	0.5
Boreal forest	750	0.0	0.12	830	6.4	4	4	2.6	1.3	0.5
Coniferous forest	1840	11.2	0.27	1058	3.8	2.6	2.2	1.4	0.7	0.25
Deciduous forest	1485	8.8	0.32	1070	1.85	1.1	0.9	0.8	0.33	0.2
Tropical forest	3210	23.6	0.78	1429	0.4	0.6	0.35	0.5	0.2	0.1

controlled by initial tissue N concentrations regardless of climate, other litter quality parameters, or site characteristics. A single, continuous nonlinear regression derived from the data explained 77% of the variability in net N immobilization and release as a function of initial leaf litter N concentrations and mass remaining for all forested biomes, humid grasslands, and tundra ecosystems (Fig. 2) (*18*). Patterns in net N immobilization and release were clearly delineated into four categories based on the initial leaf litter N concentrations (Table 1): high N (1.98% N, *Drypetes glauca*), intermediate N (1.02% N, *Quercus prinus*), low N [0.58 to 0.80% N, *Pinus resinosa* (decomposed at all but four sites), *Thuja plicata*, *Acer saccharum*], and very low N (0.39% N, *Triticum aestivum*). Litter high in initial N content had the best fit to the equation (r^2 = 0.91), although we could still explain 47% of the variation with the low-N litter that had the poorest fit. Leaf litters with intermediate to high initial N concentrations showed little or no net N immobilization, defined as the fraction of original N >1 (Fig. 2, A and B). Substantial net N release started when ~40% of the mass was lost. The maximum fraction of original N immobilized increased as the initial N concentration decreased to low and very low levels (Fig. 2, A to D). There was also a general pattern of increased variance of the fraction of N remaining as the initial N content of the leaf litter decreased. On average, 170% of the initial N was immobilized (net) in the litter with very low initial N, and net N release occurred only after 60% of the mass had been lost.

These data demonstrate that fundamental constraints on microbial physiology lead to predictable patterns in net N immobilization and release during long-term decomposition. Patterns in net N immobilization and release have been shown to be related to the initial N concentration of specific leaf litters (*19*, *20*), but these relations were thought to be dependent upon climate, other litter chemical characteristics (*7*), edaphic conditions (*21*, *22*), or microbial community composition (*23*, *24*). Theoretically the C:N ratio should dominantly control net N release during litter decomposition because microbial decomposers should only release N when their N requirements have been met. At low C:N ratios (e.g., high N concentrations), decomposers meet their N requirements directly from the litter. At higher initial C:N ratios, net immobilization typically occurs as microbes access N exogenous to the litter and convert it to microbial biomass or exoenzymes [e.g., (*25*)]. Immobilization of exogenous N is presumably controlled by N availability in the environment. Patterns in net N release and immobilization should thus be dependent upon the relative C:N ratios of the decomposer organisms and the substrate, as well as N availability in the environment. Here we show that leaf litter N dynamics can be predicted at broad spatial and long temporal scales based only on the initial litter N concentration and the mass remaining during decomposition.

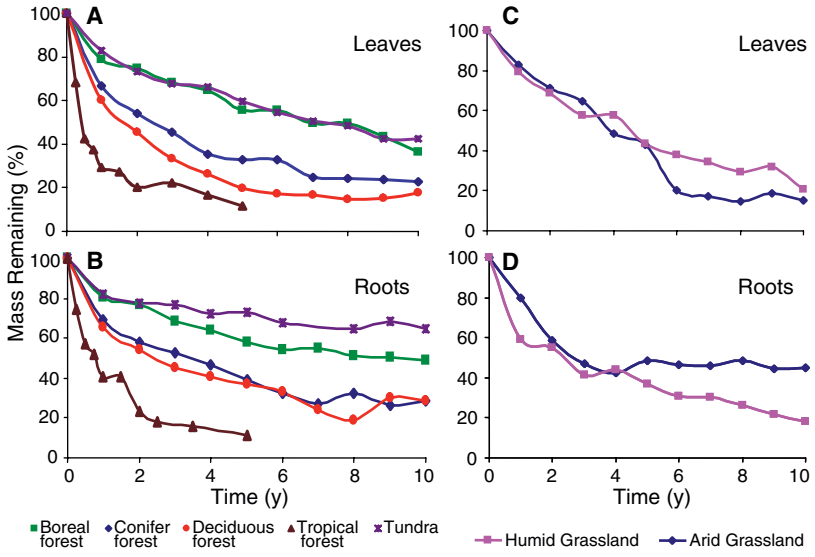

Fig. 1. Average mass remaining as a function of time for LIDET core leaf (n = 5 to 6 species) and root (n = 3 species) litters decomposed in 21 sites. (**A**) Leaf litter decomposed in forest and tundra biomes; (**B**) root litter decomposed in forest and tundra biomes; (**C**) leaf litter decomposed in humid and arid grasslands; (**D**) root litter decomposed in humid and arid grasslands. Each species and litter type was decomposed in replicate bags and collected at multiple time points. Results show that leaf and root litter decomposition rates generally increase as the CDI increases (Table 1). In arid grasslands, leaf litter decomposed more rapidly than expected (based on the CDI), possibly due to photodegradation.

Net N release started when the average C:N ratio of the leaf litter was less than 40 (a range of 31 to 48). This is somewhat lower than in a 6-year decomposition study across Canada (C:N = 55) (*22*). The Canadian study used a narrower range of initial litter N and reported no relation between initial N concentration and rates of net N release. However, when net N release and immobilization are examined per unit of mass remaining, results were similar to the LIDET study.

As with mass loss, there was one exception to the pattern of net N release from the LIDET study. In arid-zone perennial grasslands, leaf litters with low and very low initial N concentrations showed a linear trend of net N release

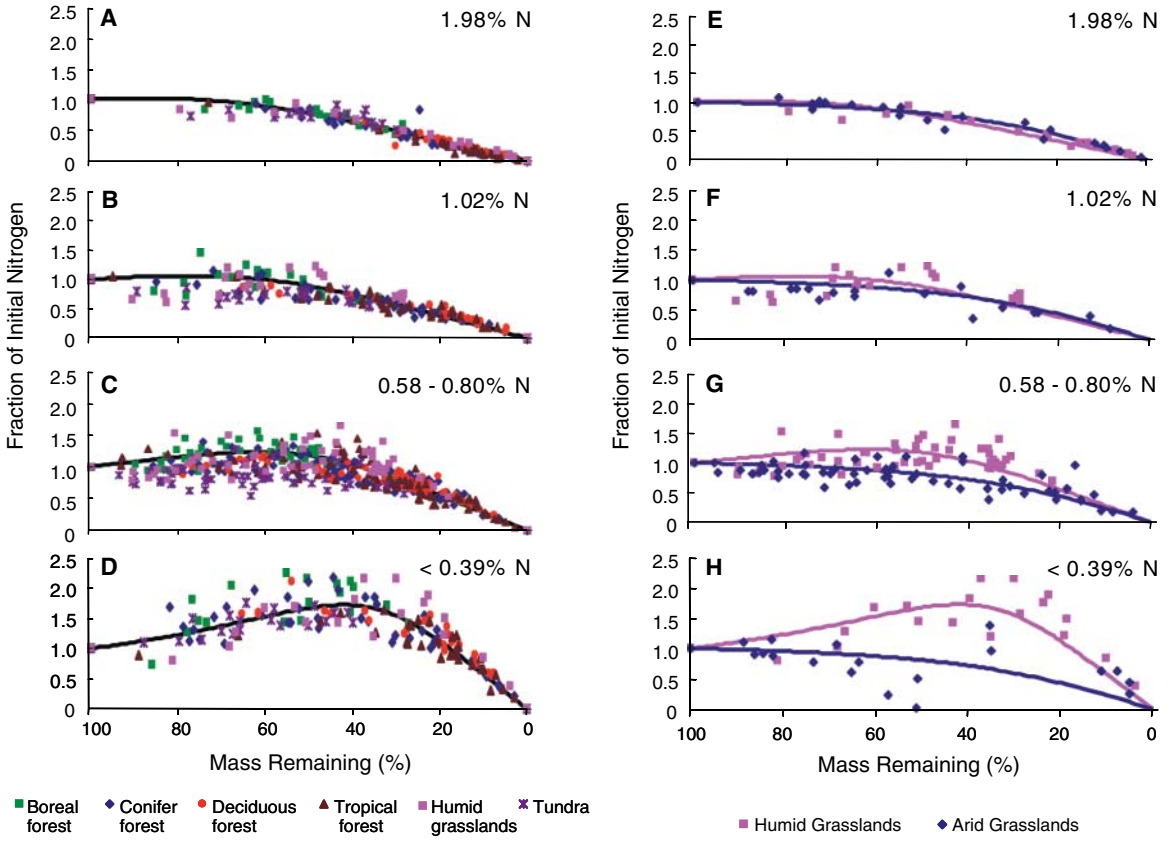

Fig. 2. Fraction of original litter N remaining as a function of the leaf litter mass remaining for tundra, grassland, and forest biomes. (**A**) to (**D**) include all biomes except arid grasslands; (**E**) to (**H**) compare arid and humid grasslands. Data are divided into litter high in initial N (A and E), intermediate initial N (B and F), low initial N (C and G), and extremely low initial N (D and H). The lines on the graphs show the best-fit model for describing the pattern of fraction of original N as a function of the initial N concentration of the litter (*18*). Model results match the observed data and show that net N immobilization, defined as an absolute increase in N concentration of the litter, is highest for the leaf litter with very low initial N concentration and decreases to minimal values for high initial N concentration of leaf litter. Leaf litter in arid grasslands was an exception showing no N immobilization in the low and very low N litters.

with little or no net N immobilization (Fig. 2, E and F). The pattern of net N release versus mass remaining for arid grasslands could be described by an equation with no effect of initial litter N concentration (*18*) (Fig. 2, E to H). This contrasts with the results from humid grasslands that exhibited increasing net N immobilization as the initial N concentration of the leaf litter decreased (Fig. 2, E to H). Leaf litters decomposed faster in humid grasslands than in arid grasslands during the early stages of decomposition, but decomposition increased more rapidly in arid grasslands after the first 3 to 5 years to a level equivalent to that of deciduous forests (Fig. 1). This was surprising given that the CDI for arid grasslands is <50% that of the humid grassland and deciduous forest biomes. The effect was not seen for root tissues, which were decomposed below ground and decayed faster in humid grasslands than in arid grasslands (Fig. 1D). The rapid increase in leaf litter decomposition during the later stages of decomposition and the linear net N release regardless of initial N concentration in arid grasslands may be caused by photodegradation. Arid grasslands typically have less than 100 g m^{-2} of standing live and dead plant tissues, whereas humid grasslands have more than 400 g m^{-2} aboveground plant biomass that intercepts most of the solar radiation before it gets to the surface leaf litter (*26*). Studies conducted during the early stages of decomposition (1 to 3 years) in arid grasslands have produced conflicting results regarding the effects of UV radiation on decomposition processes (*15*, *27*, *28*). However, recent studies suggest that where biotic decomposition is not favored (such as high litter lignin:N ratio and low moisture availability typical of arid grasslands), the abiotic process of photodegradation may predominate (*16*). This mechanism could explain the lack of a strong correlation between N concentration and decomposition, as well as the absence of net N immobilization at these sites.

Contrary to patterns of net N immobilization and release with mass loss, the time required to initiate net N release (TNET) was sensitive to initial tissue chemistry and climate. The TNET was inversely correlated with initial litter N and CDI ($r^2 = 0.77$, $P < 0.01$) (Table 1). The relation with CDI reflects the climatic controls on decomposition rate. The humid tropical biome had the lowest TNET values, ranging from 0.5 year for very low initial N litter to less than 0.1 year for high initial N litter. In the tundra and boreal forest biomes, it took more than 7 years for net N release to occur in litter with very low initial N, but only 0.5 year for net N

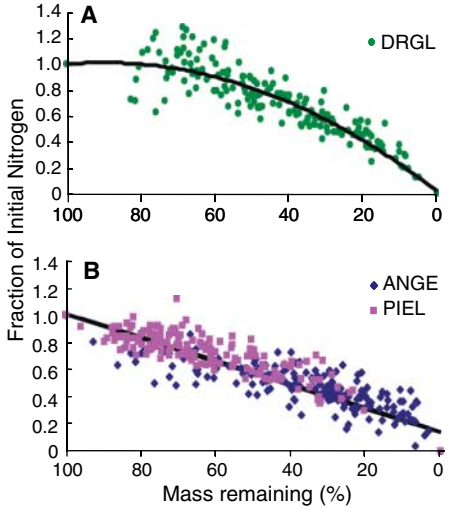

Fig. 3. Fraction of original root litter N remaining as a function of the litter mass remaining for *Drypetes glauca* root litter (**A**), and *Andropogon gerardi* and *Pinus elliottii* root litter (**B**), decomposing at the LIDET sites. Net N immobilization was minimal for decomposing root litter, with N being released as soon as decomposition of root litter starts. The equation for the DRGL roots is $y = -0.0001x^2 + 0.0221x + 0.0192$, $r^2 = 0.90$; the relation for the PIEL and ANGE roots is $y = 0.0087x + 0.1409$, $r^2 = 0.87$.

release from litter high in initial N. The TNET was at least 50% faster for most leaf litters decomposed in temperate deciduous forests when compared to coniferous forests and humid grasslands, all with similar CDIs (Table 1). Within a given CDI level, other factors such as edaphic conditions or decomposer communities may contribute to the differences observed (*29*, *30*). At the highest leaf litter N concentrations, all biomes experienced net N release during the first year of decomposition.

Root litter N followed a linear pattern with mass remaining (Fig. 3) and could best be described by two equations. The first was for *D. glauca* roots, which demonstrated a small amount of net N immobilization early in decomposition for a range of sites, possibly due to slightly higher concentrations of nonpolar extractives and slightly lower acid extractable carbohydrates concentrations than the other species (table S2). The second equation described net N release for the pine and grass roots that did not immobilize N during decomposition. A comparison of litter N dynamics during decomposition of pine and grass roots with leaf litter of similar initial N concentration (Figs. 2 and 3) showed that N was released from roots much more rapidly than from leaf litter. Roots released N as soon as litter decomposition was initiated (C:N ratio > 50). Microbial decomposers in the soil may have greater access to moisture, organic matter, and mineral N than microbes involved in leaf litter decomposition at the soil surface, which would facilitate net N release during decomposition (*31*). Similar patterns in net N release in roots have been described for native root litter decomposed in situ in grasslands (*32*), temperate broadleaf forests (*33*), temperate conifer forests (*34*), and moist and humid tropical forests (*35*, *36*).

Our data show that the initial N concentration of leaf litter is a dominant driver of net N immobilization and release during long-term litter decomposition at a global scale. This occurs regardless of climate, other litter chemical properties, edaphic conditions, or soil microbial communities. Our data also show that N can be released early in decomposition from high-quality litters in environments that support low decomposition rates. The time required to initiate net N release was predicted from the initial N of the litter and the CDI across biomes, but required more site information within a given CDI. Roots generally lost N linearly with mass loss during decomposition. Because N release during decay plays a fundamental role in net ecosystem production, improved understanding of the controls on net N release during decomposition is likely to greatly improve our ability to predict terrestrial C dynamics at global and regional scales.

References and Notes

1. H. L. Gholz, D. Wedin, S. Smitherman, M. E. Harmon, W. J. Parton, *Global Change Biol.* **6**, 751 (2000).
2. I. C. Prentice *et al.*, in *Climate Change 2001: The Scientific Basis: Contribution of Working Group I to the Third Assessment Report of the Intergovernmental Panel on Climate Change*, J. T. Houghton *et al.*, Eds. (Cambridge Univ. Press, Cambridge, 2001), pp. 183–231.
3. B. Moore, B. H. Braswell, *Ambio* **23**, 4 (1994).
4. W. S. Currie, *Global Change Biol.* **9**, 919 (2003).
5. P. M. Vitousek, R. W. Howarth, *Biogeochemistry* **13**, 87 (1991).
6. J. D. Lousier, D. Parkinson, *Can. J. For. Res.* **9**, 449 (1979).
7. B. Berg, C. McClaugherty, *Can. J. Bot.* **67**, 1148 (1989).
8. B. Berg, *For. Ecol. Manage.* **133**, 13 (2000).
9. J. D. Aber, J. M. Melillo, C. A. McClaugherty, *Can. J. Bot.* **68**, 2201 (1990).
10. R. Aerts, *Oikos* **79**, 439 (1997).
11. G. Cadisch, K. E. Giller, Eds., *Driven by Nature: Plant Litter Quality and Decomposition* (CAB International, Oxon, UK, 1997).
12. Long-Term Intersite Decomposition Experiment Team (LIDET), *Meeting the Challenges of Long-Term, Broad-Scale Ecological Experiments* (Publication No. 19, U.S. Long Term Ecological Research Network Office, Seattle, WA, 1995).
13. W. M. Post, J. Pastor, *Clim. Change* **34**, 253 (1996).
14. D. L. Moorhead, W. S. Currie, E. B. Rastetter, W. J. Parton, M. E. Harmon, *Global Biogeochem. Cycles* **13**, 575 (1999).
15. J. Rozema *et al.*, *Plant Ecol.* **128**, 284 (1997).
16. V. A. Pancotto, O. E. Sala, T. M. Robson, M. M. Caldwell, A. L. Scopel, *Global Change Biol.* **11**, 1982 (2005).
17. A. T. Austin, L. Vivanco, *Nature* **442**, 555 (2006).
18. Materials and methods are available as supporting material on *Science* Online.
19. E. H. Richards, A. G. Norman, *Biochem. J.* **25**, 1769 (1931).
20. J. D. Aber, J. M. Melillo, *Can. J. Bot.* **60**, 2263 (1982).
21. S. E. Hobbie, P. M. Vitousek, *Ecology* **81**, 1867 (2000).
22. T. R. Moore, J. A. Trofymow, C. E. Prescott, J. Fyles, B. D. Titus, *Ecosystems* **9**, 46 (2006).
23. M. H. Beare *et al.*, *Ecol. Monogr.* **62**, 569 (1992).
24. S. D. Frey, M. Knorr, J. L. Parrent, R. T. Simpson, *For. Ecol. Manage.* **196**, 159 (2004).
25. S. D. Frey, E. T. Elliott, K. Paustian, G. A. Peterson, *Soil Biol. Biochem.* **32**, 689 (2000).
26. D. S. Schimel *et al.*, *Ecology* **72**, 672 (1991).
27. H. A. Verhoef, J. M. H. Verspagen, H. R. Zoomer, *Biol. Fertil. Soils* **31**, 366 (2000).
28. S. A. Moody *et al.*, *Plant Ecol.* **154**, 27 (2001).
29. J. D. Aber, J. M. Melillo, K. J. Nadelhoffer, C. A. McClaugherty, J. Pastor, *Oecologia* **66**, 317 (1985).
30. J. E. Barrett, R. L. McCulley, D. R. Lane, I. C. Burke, W. K. Lauenroth, *J. Veg. Sci.* **13**, 383 (2002).
31. W. L. Silver, R. K. Miya, *Oecologia* **129**, 407 (2001).
32. T. R. Seastedt, W. J. Parton, D. S. Ojima, *Can. J. Bot.* **70**, 384 (1992).
33. M. E. Dornbush, T. M. Isenhart, J. W. Raich, *Ecology* **83**, 2985 (2002).
34. H. Chen, M. E. Harmon, J. Sexton, B. Fasth, *Can. J. For. Res.* **32**, 320 (2002).
35. W. L. Silver, K. A. Vogt, *J. Ecol.* **8**, 729 (1993).
36. W. L. Silver *et al.*, *Global Change Biol.* **11**, 290 (2005).
37. W. J. Parton, D. S. Schimel, D. S. Ojima, C. V. Cole, in *Quantitative Modeling of Soil Formation Processes*, R. B. Bryant, R. W. Arnold, Eds. (SSSA Special Publication 39 ASA, CSSA, and SSA, Madison, WI, 1994), pp. 147–167.

38. The LIDET study was supported by NSF Ecosystems Studies grants BSR-8805390 and BSR-9180329 to Oregon State University, NSF Shortgrass Steppe LTER grant DEB-350273, NSF IRC grant DEB-9977066, and University of Tennessee–Battelle, LLC (U.S. Department of Energy) subcontract grant 4000050162. This work was conducted as part of the Long-Term Intersite Decomposition Working Group supported by the National Center for Ecological Analysis and Synthesis, a Center funded by NSF (grant DEB-0072909), University of California, Santa Barbara. W.S. was also supported by NSF grants DEB-0218039, DEB-0219104, and the California Agricultural Experiment Station (7069-MS). W.P. was supported by DOE ORNL grant 533906, NSF grant DEB-0217631, and the NSF UV radiation project at the University of Minnesota. We thank H. Gholz for invaluable input on previous versions of this manuscript, and S. Lutz, C. Keough, and L. Richards for assistance in analyzing the extensive LIDET litter decay data set.

Supporting Online Material

www.sciencemag.org/cgi/content/full/315/5810/361/DC1
Materials and Methods
Tables S1 to S3
References

7 September 2006; accepted 5 December 2006
10.1126/science.1134853

Water Solubility in Aluminous Orthopyroxene and the Origin of Earth's Asthenosphere

Katrin Mierdel,[1] Hans Keppler,[1,2]* Joseph R. Smyth,[2,3] Falko Langenhorst[2,4]

Plate tectonics is based on the concept of rigid lithosphere plates sliding on a mechanically weak asthenosphere. Many models assume that the weakness of the asthenosphere is related to the presence of small amounts of hydrous melts. However, the mechanism that may cause melting in the asthenosphere is not well understood. We show that the asthenosphere coincides with a zone where the water solubility in mantle minerals has a pronounced minimum. The minimum is due to a sharp decrease of water solubility in aluminous orthopyroxene with depth, whereas the water solubility in olivine continuously increases with pressure. Melting in the asthenosphere may therefore be related not to volatile enrichment but to a minimum in water solubility, which causes excess water to form a hydrous silicate melt.

Earth's asthenosphere is often assumed to roughly coincide with the low-velocity zone, a layer of reduced seismic velocities and increased attenuation of seismic waves. The low-velocity zone usually begins at a depth of 60 to 80 km below the oceans and ends around 220 km (*1*). Below continental shields, the upper boundary is depressed to 150 km. The seismic characteristics of the low-velocity zone could be easily explained by the presence of a small frac-

Correction: 19 January 2007

www.sciencemag.org/cgi/content/full/315/5810/361/DC1

Supporting Online Material for

Global-Scale Similarities in Nitrogen Release Patterns During Long-Term Decomposition

William Parton, Whendee L. Silver, Ingrid Burke, Leo Grassens, Mark E. Harmon, Bill Currie, Jennifer King, E. Carol Adair, Leslie Brandt, Steve Hart, Becky Fasth

Published 19 January 2007, *Science* **315**, 361 (2007)
DOI: 10.1126/science.1134853

This PDF file includes:

Correction: The originally posted supporting online material was an early draft that was posted in error.

Supporting Online Material

Material and Methods

Nitrogen Release Formulas

We used a set of formulas to describe the patterns of N remaining in leaf litter as a function of initial N concentration (N_i in percent) and the mass remaining in the litter. The function we selected is used in Control Systems Theory to represent the error signal in the frequency domain (*S1*). We needed a function where the *"y"* value is 0 when litter biomass is 0, equal to 1.0 when litter mass is 100%, and allows for peak values of the function to be greater than 1.0. These features were needed to describe the observed patterns in the fraction of N remaining as a function of initial N concentration of the litter (%) and mass remaining (see Fig. 2 in the main text). This basic function is shown in Formula S1:

$$F(x,a,b) = \frac{x/b}{\sqrt{(2*a*x/b)^2 + (1-(x/b)^2)^2}} \qquad \text{(Formula S1)}$$

where *"a"* is the control factor for the peak value of the function, *"b"* is the location for the peak value of the function, and *"x"* is the percentage of the initial mass remaining in the litter bag (0 to 100%). We used a version of Formula S1 to describe the combined observed data from the boreal, coniferous, deciduous, and tropical forests, tundra, and wet grassland biomes. The equations we used to describe the combined data sets (data in Fig. 2A-D) are shown in Formulas S2 and S3:

$$N(x,N_i) = \frac{F(x,a,b)}{F(100,a,b)} \text{ with } a = 0.7 \qquad \text{(Formula S2)}$$

$$b = 98(1-e^{-1.56*N_i}) \qquad \text{(Formula S3)}$$

where $N(x, N_i)$ is the fraction of N remaining in the litter as a function of initial N concentration and the mass remaining in the litter for the combined data sites. We derived the parameter values in Formulas S2 and S3 by optimizing for the highest r^2 of the model values versus the observed data using a linear regression. Formula S3 describes the observed change in the *"x"* location of maximum net N immobilization for different initial litter N concentrations. The *"x"* location increases from 43% mass remaining for initial N concentrations of 0.38% N to 94% mass remaining with a 2% initial litter N concentration. The r^2 value for the combined data set (temperate conifer, boreal, deciduous, and tropical forests, chaparral, tundra, and wet grassland biomes) is 0.77; the r^2 value ranged from a low of 0.47 for litter with low initial N concentration (0.59-0.80%) to a high of 0.91 for litter with the highest initial N concentration (shown in Fig. 2 of the main text).

For the arid grassland sites, a single equation (Formula S4) could be used to represent the pattern of net N release as a function of mass remaining in the litter without considering the initial N concentration of the litter:

$$N^{DG}(x) = \frac{N(x,a,b)}{N(100,a,b)} \text{ with } a = 2.2 \text{ and } b = 200 \qquad \text{(Formula S4)}$$

where $N^{DG}(x)$ is the fraction of N remaining as a function of mass remaining in the litter (x). The fit of the equation is fairly low ($r^2 = 0.40$) because of large variations in the observed data at low initial N concentrations.

TNET and Litter Mass Loss Formulas

Here we describe the method used to calculate the time required to initiate net N release (TNET) from the LIDET core leaf litter types. TNET is defined as the time (in years) required to reach the point of maximum net N immobilization as a function of mass remaining. The data in Fig. 2A-D (see main text) show that there is an absolute increase in the N remaining in decomposing litter as the remaining mass decreases, until maximum net N immobilization occurs. Litter decomposition beyond this point results in an absolute decrease in the total N remaining in the litter (i.e., net N release, which is effectively net N mineralization). Table S1 shows the optimized value of mass remaining when maximum net N immobilization occurs for the six core leaf litters. The time point (in years) when the maximum N immobilization is reached for the six core litter types (see Table 1 main text) is evaluated using a model developed to predict mass remaining as a function of initial litter chemistry and the Climatic Decomposition Index (CDI) for each of the LIDET sites. The model was developed using the observed mass remaining data for all of the LIDET core leaf litter types (species listed in Table S2) to optimize the parameters in the model. We used the Aikai Information Criteria (*S2*) to select the best model (over 50 different models were compared in the model comparison effort) for predicting mass remaining.

To get the best estimate of TNET for each biome and litter type, we optimized the model by site and litter species. We compared a general (un-optimized) model with a model that optimized the coefficient of CDI to achieve the best fit to the observed data. In most cases, the general model did a good job of fitting the data. However, in some cases there was a substantial improvement in TNET using the optimized coefficient of CDI. For example, at the BSF site the optimized value of TNET for ACSA litter was 1.0 year closely matching the observed data, while the standard equation gave a value of 2.5 years. The optimized and un-optimized values of TNET were considerably closer for most of the sites and litter types.

The best model was a three pool litter decay model where the initial percentage of the litter in each pool is determined by the initial litter chemistry (lignin to N ratio). The decay rate of the different pools is a function of the CDI of the site and the pool specific

decay rate. Formula S5 shows the equation for predicting mass loss as a function of time, CDI, and the initial litter chemistry:

$$ {}^{j}B_i(t) = {}^{1}M_i * \exp(k1 * CDI_j * t * {}^{i}C_j) + {}^{2}M_i * \exp(k2 * CDI_j * {}^{i}L_c * t * {}^{i}C_j) + {}^{3}M_i * \exp(k3 * CDI_j * t * {}^{i}C_j) \quad \text{(Formula S5)} $$

where ${}^{j}B_i(t)$ is the biomass remaining for the "i" LIDET core litter, decomposing at the "j" LIDET site as a function of time since decomposition has started "t" (y); ${}^{1}M_i$ is the initial percentage of "i" th leaf litter in the rapid decomposition pool; ${}^{2}M_i$ is the initial percentage of the "i" th leaf litter in the cellulose pool; ${}^{3}M_i$ is the initial percentage of the "i" th leaf litter in the slowly decomposing pool (lignin pool), k1 (2.82), k2 (0.25), and k3 (0.14) are the decay rates (y^{-1}) for the three pools; ${}^{i}L_c$ is the initial cellulose to lignin ratio for the "i" th common litter (equal to ${}^{2}M_i/{}^{3}M_i$); C_j^i is the optimized CDI multiplier for the "j" th site and "i" th litter type; and CDI_j is the climatic decomposition index for the "j" LIDET site. The initial litter chemistry for the "i" th litter type is shown in Table S2; C_j^i and CDI_j values for each site and litter type are shown in Table S1. C_j^i values were determined by optimizing the value for each site and litter type so that Formula S1 best fits the observed mass remaining data for each site and litter type. The initial percentage of the mass in the three different pools is calculated using Formula S6, S7, and S8:

$$ {}^{1}M_i = 90.0 - 1.4 * {}^{i}L_N \quad \text{(Formula S6)} $$

$$ {}^{2}M_i = (1 - {}^{1}M_i) - {}^{3}M_i \quad \text{(Formula S7)} $$

$$ {}^{3}M_i = L_i \quad \text{(Formula S8)} $$

where ${}^{i}L_N$ is the effective initial lignin to N ratio of the "i" th litter and L_i is the initial lignin concentration in percent of the "i" th litter. Formulas S6, 7, and 8 were derived using an analysis of the initial litter chemistry data from the LIDET study (*S3*).

A detailed analysis of the fit for the litter decomposition model showed that mass loss from the deciduous and humid tropical forest sites were underestimated using the generic cross-site model represented by Formulas S5-S8. Formulas S9 and S10 were derived to improve the fit of litter decay model for these sites:

$$ {}^{i}L_N = L_i / N_e^i \quad \text{(Formula S9)} $$

$$ N_e^i = N_i * E_N^i \quad \text{(Formula S10)} $$

where N_e^i is the effective initial N concentration of the "i" th litter, and E_N^i is the impact of site on N concentration :

if other than deciduous and tropical forest:

$E_N^i = 1.0$

if deciduous and tropical forest:

$$E_N^i = \left\{ \begin{array}{c} 5.0 \; if \; L_{ci} \le 0.20 \\ 2.0 + (0.4 - L_{ci}) * 15 \; if \; L_{ci} > 0.2 \le 0.40 \\ 2.0 \; if \; L_{ci} > 0.40 \end{array} \right\} \qquad \text{(Formula S11)}$$

where L_{ci} is the observed lignin to cellulose ratio (see table S2) for the “i” th litter.

Table S1. Parameter values used in calculating time to net N release. Optimized mass remaining where maximum net N immobilization occurs for LIDET core leaf litter at each site and the optimized coefficient of the Climatic Decomposition Index (CDI) for fitting observed mass remaining LIDET data for core leaf litters at each site. Mean annual precipitation and temperature are given in Table 1 of the main text and species abbreviations are defined in Table S2 below.

	Mass Remaining with Maximum Net N Immobilization						Optimized Coefficient of CDI						Mean Annual CDI
	TRAE	PIRE	THPL	ACSA	OUPR	DRGL	TRAE	PIRE	THPL	ACSA	OUPR	DRGL	
Humid Grassland													
KNZ	42	63	63	65	80	90	0.8	0.45	0.40	0.45	0.25	0.7	0.31
CDR	42	63	63	65	80	90	1.0	0.45	0.90	0.70	0.43	0.6	0.29
Tundra													
NWT	42	63	63	65	80	90	1.2	0.45	0.9	1.05	0.9	0.9	0.10
ARC	42	63	63	65	80	90	1.0	0.70	1.40	1.40	0.25	0.9	0.08
Boreal Forest													
BNZ	42	63	63	65	80	90	1.2	0.70	1.0	0.75	1.1	0.7	0.10
LVW	42	63	63	65	80	90	0.8	--	1.0	0.6	.45	0.6	0.15
Temperate Conifer Forest													
JUN	42	63	63	65	80	90	1.0	--	1.4	1.25	1.9	1.0	0.20
AND	42	63	63	65	80	90	1.0	0.65	1.4	1.0	1.4	1.0	0.23
OLY	42	63	63	65	80	90	1.4	1.2	2.3	1.35	1.4	1.4	0.23
BSF	42	63	63	65	80	90	0.5	--	0.45	0.35	0.3	0.4	0.16
UFL	42	63	63	65	80	90	1.0	0.7	1.7	0.60	1.2	0.8	0.54
Temperate Deciduous Forest													
CWT	42	63	63	65	80	90	0.7	0.7	1.0	0.90	0.8	0.7	0.41
HBR	42	63	63	65	80	90	1.1	0.8	1.2	0.80	1.2	1.2	0.28
HFR	42	63	63	65	80	90	1.0	0.8	1.2	1.2	1.5	1.0	0.26
Tropical Forest													
BCI*	42	63	63	65	80	90	1.4	--	0.90	1.0	1.0	1.3	0.78
LBS	42	63	63	65	80	90	1.4	0.4	1.2	1.0	0.8	1.0	0.89
MTV	42	63	63	65	80	90	1.8	--	1.4	1.0	1.0	1.3	0.60
LUQ	42	63	63	65	80	90	2.0	0.6	1.6	1.0	1.2	1.8	0.84

Table S2. Initial litter quality chemistry of leaf and root LIDET core litters. Names for species abbreviations are given in Table 1 of the main text. Chemical analyses are described in Gholz et al. (*S4*).

Species Symbol	Species name	Nitrogen (%)	Lignin (%)	Cellulose (%)	Lignin to Cellulose Ratio
Leaf Litter					
TRAE	*Triticum aestivum*	0.38	16.2	73.2	0.22
PIRE	*Pinus resinosa*	0.58	19.2	44.6	0.43
THPL	*Thuja plicata*	0.62	26.7	35.9	0.74
ACSA	*Acer saccharum*	0.80	15.9	27.3	0.58
QUPR	*Quercus prinus*	1.02	23.5	39.4	0.59
DRGL	*Drypetes glauca*	1.98	10.9	39.8	0.27
Root Litter					
ANGE	*Andropogon gerardii*	0.63	10.5	67.1	0.16
PIEL	*Pinus elliottii*	0.82	34.9	35.9	0.97
DRGL	*Drypetes glauca*	0.76	16.1	52.2	0.30

Table S3. LIDET sites used in the analyses of decomposition rates and the patterns in litter N dynamics. Biomes refer to the location where litter bags were decomposed.

SITE	SITE CODE	Latitude	Longtitude	Biome
H.J Andrews Experimental Forest	AND	44°14' N	122°11' W	Temperate Coniferous Forest
Toolik Lake	ARC	63°38' N	149°34' W	Tundra
Barro Colorado Island	BCI	9°10' N	79°51' W	Tropical Forest
Bonanza Creek Experimental Forest	BNZ	64°45' N	148°00' W	Boreal Forest
Blodgett Research Forest	BSF	38°52' N	105°38' W	Temperate Coniferous Forest
Cedar Creek Natural History Area	CDR	45°24' N	93°12' W	Humid Grassland
Central Plains Experimental Range	CPR	40°49' N	104°46' W	Arid Grassland
Coweeta Hydrological Laboratory	CWT	35°00' N	83°30' W	Temperate Deciduous Forest
Hubbard Brook Experimental Forest	HBR	43°56' N	71°45' W	Temperate Deciduous Forest
Harvard Forest	HFR	42°40' N	72°15' W	Temperate Deciduous Forest
Jornada Experimental Range	JRN	32°30' N	106°45' W	Arid Grassland
Juneau, Alaska	JUN	58°00' N	134°00' W	Temperate Coniferous Forest
Konza Prairie Research Natural Area	KNZ	39°05'	96°35' W	Humid Grassland
La Selva Biological Station	LBS	10°00' N	83°00' W	Tropical Forest
Luquillo Experimental Forest	LUQ	19°00' N	66°00' W	Tropical Forest
Loch Vale Watershed	LVW	40°17' N	105°39' W	Boreal Forest
Monteverde Cloud Forest Reserve	MTV	10°18' N	84°48' W	Tropical Forest
Niwot Ridge/Green Lakes Valley	NWT	40°03' N	105°37' W	Tundra
Olympic National Park	OLY	47°50' N	122°53' W	Temperate Coniferous Forest
Sevilleta National Wildlife Refuge	SEV	34°29' N	106°40' W	Arid Grassland
University of Florida	UFL	29°30' N	82°15' W	Temperate Coniferous Forest

References

S1. R. C. Dorf, *Modern Control Systems* (Prentice Hall, Upper Saddle River, NJ, 2001) Third Ed.

S2. S. J. DelGrosso, A. R. Mosier, W. J. Parton, D.S. Ojima, *Biogeochemistry* **73**, 71 (2005).

S3. W. J. Parton, D. S. Schimel, D. S. Ojima, C. V. Cole in *Quantitative Modeling of Soil Formation Processes,* R B Bryant and R. W. Arnold, Eds. (SSSA Special Publication 39 ASA, CSSA, and SSA Madison WI, 1994), pp. 147-167.

S4. H. L. Gholz, D. Wedin, S. Smitherman, M. E. Harmon, W. J. Parton, Global Change Biol. 6, 751 (2000).